INTERNATIONAL JOURNAL OF AUTOMOTIVE SCIENCE AND TECHNOLOGY

2022, VOL. 6, NO: 1, 39-48 www.ijastech.org e-ISSN: 2587-0963

Experimental Investigation of Frictional Power Apportionment of Moving Parts in a Hydrogen Fueled Multi-Cylinder Spark Ignition Engine

Akshey Marwaha[1], K.A. Subramanian[1*]

0000-0001-9356-6393, 0000-0003-2610-9680

[1]*Engines and Unconventional Fuels Laboratory, Department of Energy Science and Engineering, Indian Institute of Technology Delhi, New Delhi, India*

Abstract

This study deals with the frictional power of each moving part in hydrogen fueled multi-cylinder spark ignition engine. The moving parts such as piston, rings, bearings, cam, and roller follower are considered for this study. The engine was run at a constant speed of 1500 rpm with different loads. The indicated power of the engine is calculated using the in-cylinder pressure data, and the brake power is measured with respect to different loads. The frictional power of each moving component is calculated using the models available in the literature. The constants of the models are calibrated for the engine with the input of the measured experimental data. The frictional power of the components increases with an increase in the engine's load. The friction between the piston and the ring with the liner is the highest among other components' friction due to mainly gas pressure (in the piston rings) acting on the piston being the highest. The percentages of frictional power of each moving component at the power output of 15.1 kW are 30.8% (friction in piston rings due to gas pressure), 18.4% (piston skirt), 13.4 % (bearings), 8.5 % (cam), 6.9 % (piston ring tension) at applied engine load of 15.1 kW. This study results could be useful to find avenues for reducing the friction of the moving parts to enhance the fuel economy and endurance life of the engines.

Keywords: Friction, Hydrogen, Load, Lubricating oil, Speed

Research Article

https://doi.org/10.30939/ijastech..999354

Received 22.09.2021
Revised 18.01.2022
Accepted 26.01.2022

* Corresponding author

K.A. Subramanian

subra@dese.iitd.ac.in

Address: Department of Energy Science and Engineering, Indian Institute of Technology Delhi, New Delhi, India

1. Introduction

Hydrogen is a sustainable fuel that can be derived from renewable energy sources such as solar, wind, and biomass. Hydrogen is generally produced through an electrolysis process with the input of electricity and water; steam reforming method with biomass, sulfur-iodine cycle, and chlorine-iodine cycle with water. Various ways to produce hydrogen include renewable energy sources: alkaline water electrolysis (marine sector), PEM (Proton Exchange Membrane) water electrolysis, wind and solar power, biomass, and photocatalytic energy. As the octane number of hydrogen is more than 120, it is more suitable for spark ignition engines/vehicles. Hydrogen is a carbon-free fuel, and its utilization in combustion engines results in zero carbonaceous emissions. The thermal efficiency of the hydrogen-fuelled internal combustion engines is higher than that of gasoline fuelled engines due to better combustion due to lower irreversibility in combustion [1]. The irreversibility due to friction is one of the main factors to reduce the efficiency of the hydrogen-fuelled spark ignition engine. Hence, it is essential to study the frictional losses of the hydrogen-fuelled engine to identify energy efficiency improvement. Improvement of energy efficiency is always a prime focus for internal combustion (IC) engines. Even though many factors negatively contribute to the loss of thermal efficiency of the engines, friction loss is one of the most factors for the loss in efficiency. The internal combustion engines work with many moving parts such as cam, pushrod, rocker arms, exhaust valves, piston, rings, bearings, timing gears, etc. The moving parts of the accessories need more power to overcome the friction resulting in lower efficiency as given in Table 1. The piston is considered as sliding friction where the piston cylinder and piston rings interact with the liner. Journal bearings are considered as rotating friction. Cams are also rotating friction when it lifts the pushrod. Table 1 shows the details of the moving parts of the engine.

The absolute friction work in the engine is the difference between the actual power developed inside the engine and the actual power available on the shaft. Increasing the brake mean effective pressure or engine speed enhances the power output and power density, but this

affects friction and lubrication demands, wear, efficiency, cooling load, and emission. The friction power is a function of speed, in-cylinder pressure and temperature, and intermediate products formed during combustion. The total friction work per cycle of an engine varies with respect to speed as given in Eq.1 [2].

Table 1. Details of moving parts of the engine with its accessories.

S. No.	Name of the moving parts	Type of friction
1.	Piston (rings and skirt with respect to cylinder liner)	Sliding
2.	Journal Bearing (Crankshaft and connecting rod bearings)	Rotating
3.	Cam	Rotating
4.	Roller follower	Rolling

$$W_{tf} = C_1 + C_2N + C_3N^2 \quad (1)$$

where C_1, C_2, *and* C_3 are the constants, N is the engine speed (revolutions/min).

The friction under motoring mode for 4-cylinder SI engines with respect to engine speed is given in Eq. (2)

$$tfmep(bar) = 0.97 + 0.15\left(\frac{N}{1000}\right) + 0.05\left(\frac{N}{1000}\right)^2 \quad (2)$$

where, N is the engine speed (rpm).

Motoring friction losses are different from the firing frictional losses as the latter involves the combustion gas pressure loading on piston, higher piston and cylinder liner temperatures, and the exhaust blowdown phase at the start of the exhaust process [3]. The total friction work in IC engines is the summation of three components: (i) Mechanical rubbing friction, (ii) Pumping, (iii) Accessories. The mechanical friction consists of friction from the moving parts such as piston, rings, crankshaft, and valve train. Pistons and rings contribute to approximately half of the total engine friction [4]. Pumping work includes the intake of fresh charge and expelling the burnt products during the gas exchange process. The accessory work consists of the power required for the operation of the oil pump, fuel pump, water pump, alternator, cooling fan, belts, and gears. Friction from various parts and accessories of an engine account for the frictional losses, which are difficult to overcome and not easy to evaluate due to the wide variation in magnitude of friction forces. Silveira et al. [5] conducted a study to analyse the engine frictional losses in which the total friction power amounted to 10% of the developed engine power. Kouremenos et al. [6] developed a friction model to predict the mechanical losses at elevated combustion pressures, varying speed, and load changes. The friction mean effective pressure varied linearly with the maximum combustion pressure in the study. Taraza et al. [7] developed a global friction model for multi-cylinder diesel engines with the inputs based on geometric parameters, operating conditions, and the physics governing the friction. The model successfully simulated the mechanical losses in the engine operating at steady-state and transient conditions. Livanos and Kyrtatos [8] developed a model using a medium-speed marine diesel engine data. The model predicted the effect of load and engine speed on friction losses. Taraza et al. [9] developed a global friction model for diesel engines using simplified models of main friction components (piston ring assembly, bearings, valve train, injection pump, oil pump, coolant pump). The model was applied to a four-cylinder diesel engine which showed good agreement under steady-state and transient conditions. Zweiri et al. [10] developed a friction model for a single-cylinder diesel engine to determine the instantaneous friction of components (piston assembly, bearing, valve train, and auxiliaries). The friction equations in the model were based on the theoretical calculations for hydrodynamic and mixed lubrication. The simulated results showed an accuracy of more than 97% compared with the experimental data.

Kamil et al. [11] developed a computer model (MATLAB code) to estimate the friction in individual components in a spark-ignited engine. The piston, crankshaft, valvetrain, pumping, and auxiliary losses contributed 36%, 9%, 16%, 27%, and 13%, respectively, to the total frictional power of the engine. The piston system accounts for most of the total engine friction. Zhou et al. [12] mentioned that the contribution of the piston and main bearings to engine friction increases from 40% at low speeds to 60% at 6000 rpm. Mufti et al. [13] compared the experimentally measured piston assembly friction (using indicated mean effective pressure) with a simplified piston assembly friction model. The piston skirt friction was predicted using a simple concentric piston-cylinder model and by a method including the piston's secondary motion. It was observed from the study that the simplified friction model showed realistic results. A simplified analytical friction model to predict instantaneous friction and tested on a single-cylinder SI engine by Livanos [14]. The model was compared with semi-empirical friction formulas. A good agreement was obtained in the study between simulation and experimental results, indicating that the model predicted the dynamic behavior of the engine. Fujii et al. [15] used SI motorcycle engine to develop a total friction model using engine component dimensions such as cylinder bore, piston stroke, crank pin, and journal diameters. The empirical equation for total engine friction was derived to estimate and reduce the total engine friction. Sethu et al. [16] carried out a study to measure the in-cylinder engine friction using the instantaneous IMEP method. The piston assembly friction for motoring and firing was obtained using the method. It was observed that the ratio of in-cylinder friction mean effective pressure to total engine friction mean effective pressure ranged from 19-44% and 26-42%, when motored without and with spark plugs, respectively.

Very few studies are available on calculating friction in natural gas-fueled engines. It was mentioned in a study that SI CNG fueled engine has a 25% higher friction factor than CI diesel due to the throttling valve [17]. Orbaiz et al. [18] carried out a comparative study of SI engine running on hydrogen and natural gas. It was observed that the increasing load significantly reduced the pumping losses due to reduced throttling, whereas increasing engine speed increased both friction and pumping losses. The pumping friction losses (as percentage fuel energy) were observed to be higher with natural gas compared to hydrogen at the experimental operating conditions (1500 rpm and 83 Nm, 1500 rpm and 140 Nm,

3500 rpm and 83 Nm). Wong et al. [19] conducted a study to improve the efficiency of natural gas engines by reducing piston and piston assembly friction. The use of low friction lubricants showed a total engine FMEP reduction of up to 16.5%. It was observed that flat piston led to significant friction reduction.

Hydrodynamic friction constitutes a significant fraction of friction losses, indicating that reduced viscosity can result in lower frictional losses. However, the metal-to-metal contact severity is significantly increased when lubricant viscosity is reduced [2]. Ting and Shih [20] mentioned that for firing conditions, metal-to-metal contact friction is dominant due to high gas pressure and high oil film temperature and reduced oil viscosity, leading to reduced oil film thickness. The challenge is to balance the reduction in viscous frictional losses obtained with low viscosity fluids with the increase in friction and contact severity (wear and failure) associated with such fluids [21]. Different grades of oil are developed to deliver optimum performance at the required temperatures. Thus, the combustion temperature plays a vital role in the selection of oil for different applications as viscosity is highly temperature-dependent. Nada et al. [22] mentioned that an engine with lubricating oils with higher viscosity lowers thermal efficiency. Takata and Wong [23] studied the effect of lubricant viscosity on piston ring-liner friction. It was concluded from the study that the oil viscosity at piston movement in the middle of the total volume (mid-stroke) dominates the overall frictional losses (hydrodynamic friction) in rings.

Viscosity index is an important characteristic of lubricating oil, defined as the rate of change of viscosity with respect to the temperature change. The viscosity index of lubricating oil is calculated according to the test method ASTM 2270 [24]. The high values of the viscosity index lead to a decrease in viscosity with temperature. The viscosity index improvers reduce the rate of change of viscosity with temperature change [25].

Continuous improvements have been made in IC engines to reduce frictional losses and enhance the performance and efficiency of the engine. Hoshi [26] reduced the frictional losses in the piston system by 23-25% by reducing the cross-sectional dimensions of piston rings and lowering their tensions. The change of conventional V-belts to multi-V-belts to drive accessories reduced the frictional losses by 1-2%. Kovach et al. [27] claimed that the piston and ring friction could be reduced through reduced ring tension and ring geometry changes. Reduced gear diameter and reduced drive ratio of oil pumps are effective in parasitic friction reduction. Hamatake et al. [28] studied the friction characteristics of piston rings and concluded that decreasing the number of piston rings results in an effective reduction of frictional loss. Rahmani et al. [29] mentioned that cylinder liner temperature is influential in mitigating frictional power loss. Increased working temperatures result in reduced viscous shear stress and subsequently reduced viscous friction (lower oil viscosity).

Various models have been developed to predict the frictional power losses in SI and CI engines. Past studies have also analyzed the apportionment of individual engine components to total engine friction. However, no study in the past is reported on the assessment of frictional power losses in a hydrogen-fuelled engine. The variation in frictional power losses with respect to engine load at constant engine speed has not been reported in the literature. The present study tries to address these research gaps in the literature. This study analyzed the sole effect of engine load on frictional power loss in constant-speed hydrogen fuelled Genset using the updated models and experimental results. The empirical model constants were calibrated to predict the actual frictional losses of each moving part of the engine.

2. Experimental details

The experimental tests were conducted on a constant speed hydrogen-fuelled multi-cylinder spark-ignition engine. The technical specifications of the Genset are given in Table 2. Figure 1 shows the multi-cylinder Genset setup used for the research work.

Table 2. Specifications of Genset.

Parameters	Value
Number of cylinders	4
Revolutions/min	1500
Bore x Stroke	105 mm x 120 mm
Compression ratio	12:1
Displacement	1038.55 cm^3

The engine was integrated with the alternator having a rated power output of 28 kW. The engine was loaded with an electrical loading panel. A piezoelectric pressure transducer mounted on the engine's cylinder head was used to collect the pressure traces. AVL Indicom software was used to post-process and analyze the in-cylinder pressure data with respect to crank angle collected by the combustion analyser. Hydrogen was injected into the engine's intake manifold using a dedicated electronic control unit. The maximum brake torque spark timing of 16ºbTDC was used in this experimental study.

3. Methodology

SAE 15W-40 grade engine lubricating oil was used in the Genset for the present study. The specification of the lubricant is given in Table 3.

Table 3. Lubricant specifications.

SAE 15W-40	
Density (g/l)	866
Kinematic Viscosity at 40°C (cSt)	107
Kinematic Viscosity at 100°C (cSt)	14.6

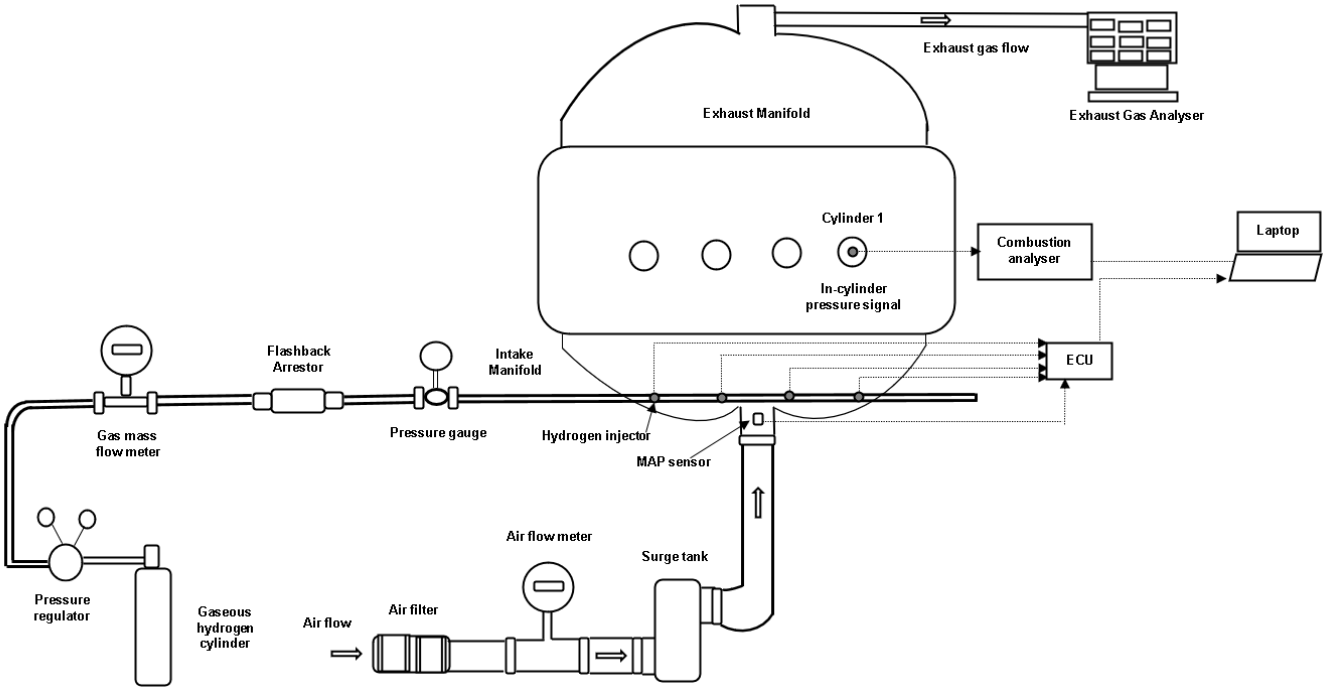

Fig. 1. Schematic layout of the experimental setup.

3.1 Mechanical performance analysis

The total mechanical friction in the engine can be computed with the summation of various mechanical rubbing parts such as the bearings, cam, piston rings, gas pressure, etc.

The empirical formulae used for the frictional power estimation are given in Eqs. (3-11) [30,31]

$$fmep_{bearings} = c_b \left(\frac{n_b N^{0.6} D_b^3 L_b}{k\, b^2 s}\right)\left(\frac{\mu}{\mu_{ref}}\right)^{0.4} \quad (3)$$

where, c_b=0.0202(kPa-min0.6/rev0.6-mm) is the constant of proportionality, n_b is the number of bearings, N is the engine speed (rpm), D_b is the bearing diameter (mm), L_b is the bearing length (mm), k is the number of cylinders, b is the bore of the cylinder (mm), s is the stroke of the cylinder (mm), μ is lubricant viscosity (mPa s), μ_{ref} is the viscosity of reference lubricant (mPa s).

The number (n_b) of bearings, diameter (D_b), and length (L_b) of bearings are 5, 69 mm, and 21.6 mm, respectively. The reference lubricant mentioned in this study is SAE 30. The dynamic viscosity of used and reference lubricant is 92.7 and 74.6 mPa s, respectively.

$$fmep_{seals} = c_s \frac{D_b}{k\, b^2 s} \quad (4)$$

where c_s=9.36 x 104 kPa-mm^2 is the constant of proportionality.

$$fmep_{skirt} = c_{ps} \frac{U_p}{b} \quad (5)$$

where c_{ps}=294 kPa-mm-s/m is the constant of proportionality, U_p is the mean piston speed (m/s). The value of mean piston speed (U_P = 2LN) is 6 m/s.

$$fmep_{rings} = c_{pr}\left(1 + \frac{1000}{N}\right)\frac{1}{b^2} \quad (6)$$

where c_{pr} =4.06 x 104 kPa-mm^2 is the constant of proportionality.

$$fmep_{gas} = c_g \frac{P_i}{P_a}\left(0.088r + 0.182r^{(1.33-KU_p)}\right) \quad (7)$$

where c_g= 6.89 is the constant of proportionality, P_i is intake air pressure, P_a is the ambient pressure, r is the compression ratio, K = 2.38 × 10^{-2} s/m.

The intake air pressure (P_i) depends on the throttle opening and the value of ambient pressure (P_a) taken is 1.01 bar.

$$fmep_{cam} = c_c \frac{N n_{cs}}{k\, b^2 s} \quad (8)$$

where c_c=6720 kPa-mm^3-min$^{0.6}$/rev$^{0.6}$ is the constant of proportionality, n_{cs} is the number of camshaft bearings. The number (n_{cs}) of camshaft bearings is 4.

$$fmep_{rf} = c_{rf} \frac{n_v N}{k\, s} \quad (9)$$

where c_{rf} =0.0076 is the roller follower coefficient and n_v is the number of valves. The number of valves in the cylinder is 2.

$$fmep_{oil\ pump} = 1.28 + (0.0079N + (-8.4x10^{-7})N^2)\left(\frac{\mu}{\mu_{ref}}\right)^{0.3} \quad (10)$$

where N is the engine speed (rpm), μ is lubricant viscosity (mPa s), μ_{ref} is viscosity of reference lubricant (mPa s).

$$fmep_{water\ pump} = 0.13 + (0.002N + 3\ \text{x}\ 10^{-7}N^2)\left(\frac{\mu}{\mu_{ref}}\right)^{0.7} \quad (11)$$

In order to account for the mechanical frictional losses in the parts of the engine, net indicated power, brake power, and the power to the auxiliaries must be accounted for the same.

$$FP\ of\ rubbing\ component = IP_{net} - BP - AFPL \quad (12)$$

where IP_{net} is the net indicated power (kW), BP is the brake power (kW) and $AFPL$ is auxiliary frictional power loss (kW).

Performance analysis

The pressure transducer was used to collect the in-cylinder pressure data for several cycles of engine operation. The indicated work done per cycle (per cylinder) is calculated using Eq. (13)

$$W_i = \oint p.dV \quad (13)$$

where, p is the in-cylinder pressure (kPa) at each crank angle, dV is the change in instantaneous volume per crank angle degree (m^3). Gross indicated work done (Joules) per cycle is obtained using Eq. (14)

$$W_{gross} = \frac{1}{V_s}\int_{-180}^{180} p.dV \quad (14)$$

where, V_s is the swept volume (m^3). Net indicated work done (Joules) per cycle can be obtained using Eq. (15)

$$W_{net} = \frac{1}{V_s}\int_{-360}^{360} p.dV \quad (15)$$

Net indicated power (Watts) can be calculated using Eq. (16)

$$P_{net} = \frac{W_{net}\ N\ k}{2 \times 60} \quad (16)$$

where, W_{net} is the net indicated work done (J), N is the engine speed (rpm), k is the number of cylinders. Gross IMEP (Pascal) is given in Eq. (17)

$$IMEP_{gross} = \frac{W_{gross}}{V_s} \quad (17)$$

where, W_{gross} is the gross indicated work done (J), V_s is the swept volume (m^3). Net IMEP (Pascal) is obtained using Eq. (18)

$$IMEP_{net} = \frac{W_{net}}{V_s} \quad (18)$$

PMEP (Pascal) is obtained using Eq. (19)

$$PMEP = IMEP_{gross} - IMEP_{net} \quad (19)$$

where, $IMEP_{gross}$ is the gross indicated mean effective pressure (Pa), $IMEP_{net}$ is the net indicated mean effective pressure (Pa).

4. Results and Discussion

The evaluation of frictional losses of individual engine components in a hydrogen-fuelled spark ignition engine is analysed using the models and experimental results. Based on the empirical formulae given in Eqs. (3) - (11) in the methodology section, FMEP is calculated for mechanical and auxiliary friction components. The mechanical rubbing friction was evaluated with the inputs indicated, brake, and auxiliary power. The indicated power was calculated with the input of pressure-crank angle data per cycle for the three loads 7.3 kW, 10 kW, and 15.1 kW. The constants of the model were calibrated to predict the actual frictional losses of the hydrogen Genset engine. The results of the study are discussed as follows:

4.1 Mechanical friction from individual engine components

The inputs of the engine geometry (bore, stroke, compression ratio, camshaft bearings, bearing diameter, bearing length, etc.), operating conditions (engine speed and intake manifold pressure), and oil viscosity were used for the evaluation of mechanical frictional losses. Figure 2 depicts the contribution of various engine components to mechanical friction observed at 7.3 kW load at 1500 rpm. Table 4 shows the frictional power loss from all the individual engine components at 7.3 kW engine load.

Piston assembly (piston skirt, piston ring tension, gas pressure in piston ring), bearings, and cam account for most mechanical friction. Piston assembly accounts for 66% of mechanical friction, whereas seals and roller followers had a negligible contribution to mechanical friction at a 7.3 kW load.

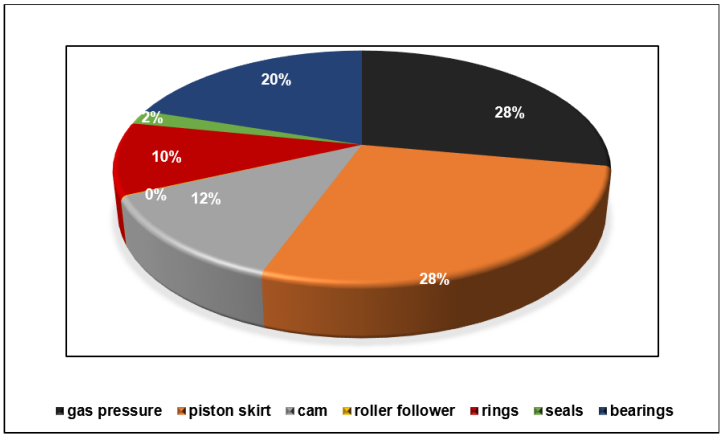

Fig. 2. Contribution of mechanical rubbing parts to friction at 7.3 kW load.

The reason for higher friction from piston assembly is due to the continuous sliding friction between the piston rings and cylinder liner for the complete cycle.

Table 4. Frictional power loss for individual friction components at 7.3 kW load.

Friction component	Friction mean effective pressure (kPa)	Frictional Power loss (kW)
Gas pressure in piston ring	17.01	0.88
Piston skirt	16.80	0.87
Cam	7.62	0.39
Roller follower	0.05	0.00
Piston ring tension	6.14	0.32
Seals	1.22	0.06
Bearings	12.07	0.63
Total	60.91	3.17

The total mechanical frictional loss from all components at 7.3 kW adds up to 3.17 kW. Similarly, the mechanical frictional loss at 10 kW and 15.1 kW is 3.25 kW and 3.73 kW, respectively. The mechanical friction from engine components increases with the engine load. The intake air pressure increases with an increase in load (0.55, 0.6, and 0.9 bar at loads 7.3, 10, and 15.1

kW, respectively) leading to a rise in peak in-cylinder pressure. Higher combustion pressures at increased engine loads have a significant influence on total mechanical friction. A study by Werner et al. [32] also mentioned that the combustion chamber pressure significantly increases the piston ring's contact pressure against the cylinder liner. Table 5 shows the increasing dominance of gas pressure (acting on piston ring) on the mechanical friction between the liner and piston ring at higher loads.

Table 5. Percentage of gas pressure to mechanical rubbing friction.

Load	In-cylinder pressure (bar)	Gas pressure contribution to mechanical friction
7.3 kW	31.5	27.9%
10 kW	35.0	29.7%
15.1 kW	46.3	38.8%

4.2 Auxiliary friction

The auxiliary friction is a function of engine speed and lubricant viscosity and is independent of the engine load. The inclusion of auxiliary friction gives the actual engine friction. The total auxiliary frictional power of the water pump and oil pump calculated in this study is 0.86 kW.

4.3 Pumping friction

The pumping friction at varying loads is calculated using the experimental pressure-crank angle data. The PMEP values are calculated by subtracting gross and net IMEP values. Figure 3 shows the variation in in-cylinder pressure and PMEP with engine load. The increasing in-cylinder pressure with load indicates the increased influence of combustion gas pressures on mechanical friction [31]. The decrease in PMEP with increased load is due to higher throttle opening (with increased load demand) leading to lower pumping losses.

4.4 Variation of frictional power loss at various loads

The frictional losses are calculated using the empirical models and compared with the experimental results. The sum of mechanical and auxiliary friction is calculated by subtracting net IMEP and BMEP. The variation in the sum of mechanical and auxiliary friction values obtained at various loads by both methods is shown in Figure 4a. The values predicted by the model are lower than the experimental results.

Figure 4b shows the trend of mechanical frictional power loss with the variation in loads. The frictional power increases with increasing loads due to the pronounced effect of increasing mechanical friction over decreasing pumping friction. The experimental FP loss is used as a reference for the comparison. The experimental data gives actual friction in the engine as it accounts for the auxiliary friction too. The empirical mechanical FP values are much lower than the actual experimental FP values. Thus, the empirical model underpredicts the actual frictional power values.

4.5 Calibration of model constants

The MMEP values calculated by empirical models and experimental results are given in Table 6. The difference in MMEP values is used to calibrate the constants of the model. Hence, the constants need to be optimized to provide the desired accuracy results. Table 7 shows the calibrated empirical model constants for the actual calculation of mechanical friction at 7.3 kW load. The mechanical frictional power losses are scaled up as per the contribution of individual components. The constants are then calibrated based on the mechanical frictional power losses. The calculated value of the actual mechanical frictional power loss at 7.3 kW from calibrated constants is 5.18 kW. The same methodology calibrates the constants for engine loads 10 kW and 15.1 kW. The actual values of mechanical frictional power loss calculated at 10 kW and 15.1 kW from the calibrated constants are 5.33 kW and 6.76 kW, respectively.

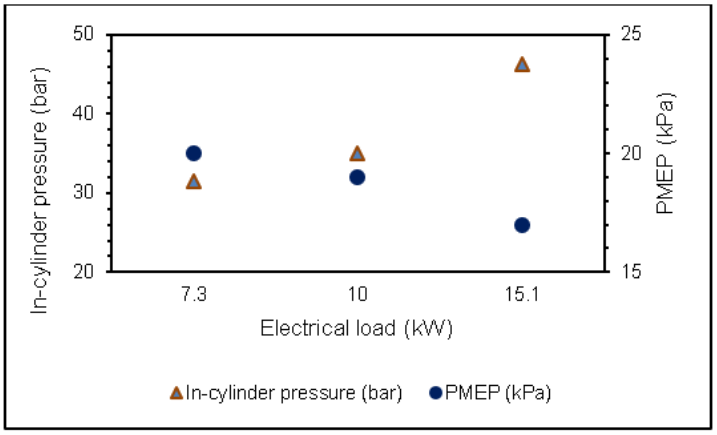

Fig. 3. Variation in in-cylinder pressure and PMEP with the load.

4.6 Calculation of total frictional power losses with calibrated constants

The obtained results are used to form an equation to calculate the total frictional power loss. The total frictional power loss is calculated using Eq. (20)

$$TFPL = MFPL + PFPL + AFPL \quad (20)$$

where *MFPL* is the mechanical frictional power loss, *PFPL* is the pumping power loss, *AFPL* is auxiliary frictional power loss. Table 8 shows the calculated mechanical and total frictional power loss at various loads. Table 9 shows the percentage of various friction components to the total frictional power loss and mechanical frictional power loss at various loads. The piston assembly contributes roughly 50% of the total engine friction. Various other researchers, such as Rakopoulos and Giakoumis [33] and Abril et al. [34], mentioned piston assembly's contribution to be 50% and 55% of the total frictional losses.

The mechanical frictional loss is dominant in the total losses in the engine and thus covers most of the total frictional power loss at higher loads (15.1 kW). The contribution of auxiliary friction to the total frictional power loss amounts to 12.1% at 7.3 kW load. The contribution reduces at higher loads (12% at 10kW load and 10.2% at 15.1kW load) due to greater significant

influence of mechanical rubbing friction. The pumping friction contribution is 14.6%, 13.6% and 10.3% at 7.3 kW, 10 kW and 15.1 kW loads, respectively. The study results could be helpful to predict the frictional power losses in an IC engine operating at a constant speed and varying loads.

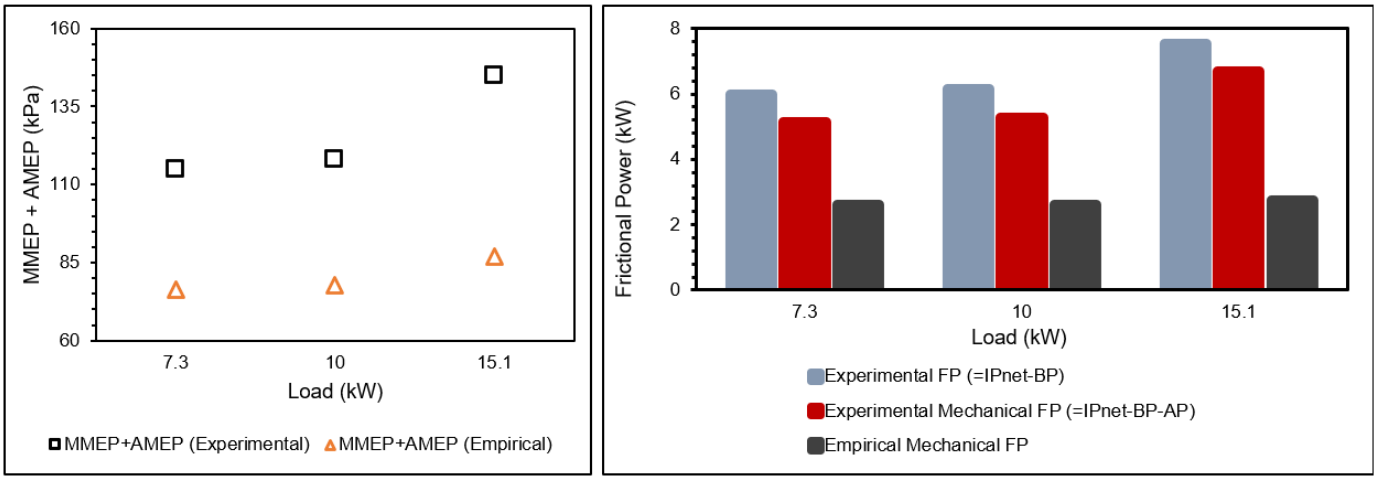

Fig. 4. a) Sum of mechanical and auxiliary friction pressure (experimental and empirical) at various loads.
b) Frictional power loss at various loads

Table 6. Empirical and experimental MMEP values.

Load (kW)	MMEP empirical (kPa)	MMEP experimental (kPa)	Difference in MMEP (kPa)	Difference in Mechanical Frictional Power loss (kW)
7.3	60.91	98.45	38.75	2.01
10	62.46	101.45	40.15	2.09
15.1	71.73	128.45	57.85	3.00

Table 7. Calibrated model constants for calculation of MMEP at 7.3 kW load.

Mechanical friction component	Older constants (Empirical model)	Older MMEP (kPa) / MFPL (kW)	Percentage (from empirical model)	Additional MMEP (kPa)	New MMEP (kPa) / MFPL (kW)	Calibrated constants
Piston skirt	c_{ps} = 294 kPa-mm-s/m	16.80 kPa 0.87 kW	28%	10.84	27.64 kPa 1.44 kW	438.5 kPa-mm-s/m
Piston ring (tension)	c_{pr} = 4.06 x 10^4 kPa-mm^2	6.14 kPa 0.32 kW	10%	3.87	10.01 kPa 0.52 kW	6.68 x 10^4 kPa-mm^2
Gas pressure (in piston ring)	c_g = 6.89	17.01 kPa 0.88 kW	28%	10.84	27.85 kPa 1.45 kW	12.2
Bearings	c_b = 0.0202 kPa-$min^{0.6}$/$rev^{0.6}$-mm	12.07 kPa 0.63 kW	20%	7.74	19.81 kPa 1.03 kW	0.035 kPa-$min^{0.6}$/$rev^{0.6}$-mm
Seals	c_s = 9.36 x 10^4 kPa-mm^2	1.22 kPa 0.06 kW	2%	0.77	1.99 kPa 0.10 kW	15.54 * 10^4 kPa-mm^2
Cam	c_c = 6720 kPa-$mm^3min^{0.6}$/$rev^{0.6}$	7.62 kPa 0.39 kW	12%	4.65	12.27 kPa 0.64 kW	10820 kPa-mm^3-$min^{0.6}$/$rev^{0.6}$
Roller follower	c_{rf} = 0.0076 kPa-mm-min/rev	0.05 kPa 0 kW	0%	-	0.05 kPa 0 kW	-
Total		60.91 kPa 3.15 kW			99.63 kPa 5.18 kW	

Table 8. Predicted frictional power loss from the calibrated model

Load (kW)	MFPL (kW)	TFPL (kW)
7.3	5.18	7.01
10	5.33	7.11
15.1	6.76	8.41

Table 9. Percentage effect of friction components to TFPL and MFPL.

Friction components	Percentage effect to TFPL (%)			Percentage effect to MFPL (%)		
	7.3 kW	10 kW	15.1 kW	7.3 kW	10 kW	15.1 kW
Piston skirt	20.3	20.0	18.4	27.7	26.9	23.1
Gas pressure (in piston ring)	20.5	22.2	30.8	28.0	29.8	38.7
Bearings	14.6	14.3	13.4	19.9	19.2	16.8
Cam	9.0	9.0	8.5	12.3	12.1	8.5
Piston ring (tension)	7.4	7.4	6.9	10.1	9.9	8.7
Seals	1.5	1.5	1.5	2.0	2.0	1.8
Roller follower	0	0	0	0.1	0.1	0
Oil pump	8.8	8.7	7.4	-	-	-
Water pump	3.3	3.3	2.8	-	-	-
Pumping (suction and exhaust)	14.6	13.6	10.3	-	-	-

5. Conclusions

The frictional apportionment of various engine components was carried out in a hydrogen-fuelled multi-cylinder spark ignition engine. The following conclusions have emerged from this study.

- The frictional power is generally calculated using the inputs of net indicated power and brake power of the engine, but it does not reflect the friction power of each moving part. In the present study, the friction power and the percentage of apportionment of each component are calculated.
- The experimental data were used to calibrate the constants of the model for the calculation of the frictional losses with reasonable accuracy.
- Friction in piston-cylinder liner due to gas pressure acting on the piston as well as pumping losses due to more throttle opening at higher loads at high load. The percentage of friction in the piston ring increases from 27.7% to 38.8% with the increase of engine load from 7.3 kW to 15.1 kW.
- The piston-cylinder assembly contributes about 50% of the total frictional power in the engine. This is due to the continuous sliding friction between the piston rings and cylinder liner during operation.
- The auxiliary friction amounts to 12.1%, 12% and 10.2% of the total engine friction at a 7.3 kW, 10 kW and 15.1 kW loads, respectively. The friction due to pumping of charge is 14.6%, 13.6% and 10.3% at 7.3 kW, 10 kW and 15.1 kW, respectively.

Appendix

The uncertainty in the measurement of engine speed was determined by calculating the standard error of the mean as given in Eq. (A.1)

$$SE = \frac{SD}{\sqrt{n}} \quad \text{(A.1)}$$

where, *SD* is the standard deviation and *n* is the number of measurements. The number of measurements is 30 and a 95% confidence level (1.96 x SE) is taken for the uncertainty analysis.

The calculated parameters ($fmep_{bearings}$, $fmep_{cam}$, $fmep_{roller\ follower}$, $fmep_{oil\ pump}$, $fmep_{water\ pump}$) depend on one independent variable, that is, engine speed. The uncertainty in these calculated terms was determined using the method given by Taylor [35] as shown in Eq. (A.2)

$$\delta r = \pm\sqrt{\left(\frac{\partial r}{\partial N} \text{ x } \delta N\right)^2} \quad \text{(A.2)}$$

where, $\partial r/\partial N$ is the differential term with respect to engine speed and δN is the uncertainty in engine speed.

The uncertainty in measured and calculated parameters is shown in Table A.1.

Table A.1. Uncertainty values in measured and calculated parameters

Parameter	Measured/Calculated	Uncertainty
Engine speed	Measured	±1.10
$fmep_{bearings}$	Calculated	±0.01
$fmep_{cam}$	Calculated	±0.56
$fmep_{roller\ follower}$	Calculated	±0.004
$fmep_{oil\ pump}$	Calculated	±0.59
$fmep_{water\ pump}$	Calculated	±0.32

Nomenclature

AFPL : Auxiliary Frictional Power Loss
ASTM : American Society for Testing and Materials
BMEP : Brake Mean Effective Pressure
BP : Brake Power
CI : Compressed ignition
CNG : Compressed Natural Gas
CoV : Coefficient of Variation
FMEP : Friction Mean Effective Pressure
FP : Frictional Power
FPL : Frictional Power Loss
ICE : Internal combustion engine
IMEP : Indicated Mean Effective Pressure
IP : Indicated Power
PFPL : Pumping Frictional Power Loss
PMEP : Pumping Mean Effective Pressure
MFPL : Mechanical Frictional Power Loss
MMEP : Mechanical Mean Effective Pressure
MP : Mechanical Power
SD : Standard Deviation
SE : Standard Error
SI : Spark ignition
SAE : Society of Automotive Engineers
TDC : Top Dead Centre
TFPL : Total Frictional Power Loss
δr : Uncertainty in calculated parameters
δN : Uncertainty in engine speed
A : Piston area (m^2)
B : Cylinder bore (mm)
c_b : Constant of proportionality for bearing friction mean effective pressure (kPa-$min^{0.6}$ /$rev^{0.6}$ -mm)
c_c : Proportionality constant for cam friction mean effective pressure (kPa-mm^3 -$min^{0.6}$ /$rev^{0.6}$)
c_{pr} : Proportionality constant for piston rings friction mean effective pressure
c_{ps} : Piston skirt friction coefficient (kPa-mm-s/m)
c_{rf} : Roller follower coefficient (kPa-mm-min/rev)
c_s : Proportionality constant for seals friction mean effective pressure (kPa-mm^2)
D_b : Bearing diameter (mm)
dV : Change in instantaneous volume (per crank angle degree)
$IMEP_{gross}$: Gross indicated mean effective pressure (Pa)
$IMEP_{net}$: Net indicated mean effective pressure (Pa)
IP_{gross} : Gross indicated power (kW)
IP_{net} : Net indicated power (kW)
k : Number of cylinders
L_b : Bearing length (mm)
n : Number of measurements
N : Engine speed (rpm)
n_b : Number of bearings
n_{cs} : Number of camshaft bearings
n_v : Total number of valves
p : In-cylinder pressure (kPa)
P_a : Ambient pressure (bar)
P_{max} : Maximum in-cylinder pressure (bar) in a cycle
P_i : Intake air pressure (bar)
P_{net} : Net indicated power (Watts)
r : Compression ratio
s : Cylinder stroke (mm)
U_p : Mean piston speed (m/s)
μ : Lubricant viscosity (mPa s)
μ_{ref} : Viscosity of reference lubricant (mPa s)
W_{net} : Net indicated work done (J)
W_{gross} : Gross indicated work done (J)

Conflict of Interest Statement

The authors declare that there is no conflict of interest in the study.

CRediT Author Statement

Akshey Marwaha: Conceptualization, Data curation, Writing
K.A. Subramanian: Conceptualization, Supervision, Editing.

References

[1] Dhyani V, Subramanian KA. Experimental based comparative exergy analysis of a multi-cylinder spark ignition engine fuelled with different gaseous (CNG, HCNG, and hydrogen) fuels. Int J Hydrogen Energy 2019; 44:20440–51.
[2] Heywood J. Internal combustion engine fundamentals. McGraw-Hill Education (1st edition),1988.
[3] Sandoval D, Heywood JB. An improved friction model for spark-ignition engines. SAE Tech. Pap., 2003.
[4] Duleep KG. Internal Combustion Engine Vehicles. Encycl Energy 2004; 3:497–513.
[5] Da Silveira MA, Gertz LC, Cervieri A, Rodrigues AFA, Senger M. Analysis of the friction losses in an internal combustion engine. SAE Tech Pap 2012.
[6] Kouremenos DA, Rakopoulos CD, Hountalas DT, Zannis TK. Development of a detailed friction model to predict mechanical losses at elevated maximum combustion pressures. SAE Tech Pap 2001.
[7] Taraza D, Henein N. Friction Losses in Multi-Cylinder Diesel Engines. SAE Tech Pap 2018.
[8] Livanos G, Kyrtatos NP. A model of the friction losses in diesel engines. SAE Tech Pap 2006.
[9] Taraza D, Henein NA, Ceausu R, Bryzik W. Engine friction model for transient operation of turbocharged, common rail diesel engines. SAE Tech Pap 2007.
[10] Zweiri YH, Whidborne JF, Seneviratne LD. Instantaneous friction components model for transient engine operation. Proc. Inst. Mech. Eng. D: J. Automob. Eng 2000:809-24.
[11] Kamil M, Rahman MM, Bakar RA. An integrated model for predicting engine friction losses in internal combustion engines. Int J Automot Mech Eng 2014.
[12] Zhou Q, Shilling I, Richardson SH. Prediction of total engine friction power loss from detailed component models. Tribol Res Des Eng Syst Proc 29th Leeds-Lyon Symp Tribol 2003:761–766.

[13] Mufti RA, Priest M, Chittenden RJ. Analysis of piston assembly friction using the indicated mean effective pressure experimental method to validate mathematical models. Proc. Inst. Mech. Eng. D: J. Automob. Eng 2008:1441-57.
[14] Livanos G. Development of a simplified instantaneous friction model of the piston-crank-slider mechanism of internal combustion engines. SAE Int. J. Engines 2011:581-96.
[15] Fujii I, Yagi S, Sono H, Kamiya H. Total engine friction in four stroke SI motorcycle engine. SAE trans 1988:419-30.
[16] Sethu C, Leustek ME, Bohac SV, Filipi Z, Assanis DN. An investigation in measuring crank angle resolved in-cylinder engine friction using instantaneous IMEP method. SAE Tech. Pap 2007.
[17] Lajevardi SM, Axsen J, Crawford C. Examining the role of natural gas and advanced vehicle technologies in mitigating CO2 emissions of heavy-duty trucks: Modeling prototypical British Columbia routes with road grades. Transp. Res. D: Transp. Environ 2018:186-211.
[18] Orbaiz P, Brear MJ, Abbasi P, Dennis PA. A comparative study of a spark ignition engine running on hydrogen, synthesis gas and natural gas. SAE Int. J. Engines 2013:23-44.
[19] Web: Low-engine-friction technology for advanced natural-gas-reciprocating engines. Massachusetts Inst. of Technology (MIT), Cambridge, MA (United States). 2006. Access: https://www.osti.gov/servlets/purl/907969
[20] Ting LL, Shih TS. Piston ring friction loss behaviour for motored and fired reciprocating engines. Lubr Sci 1995; 8:37–48.
[21] Web: Final Report for U.S. Department of Energy Fuels & Lubricants Project on Lubricant Technology – Innovation, Discovery, Design, and Engineering. Argonne National Laboratory. 2018 Jul. Access: https://publications.anl.gov/anlpubs/2019/04/146381.pdf
[22] Abu-Nada E, Al-Hinti I, Al-Sarkhi A, Akash B. Effect of piston friction on the performance of SI engine: A new thermodynamic approach. J Eng Gas Turbines Power 2008;130.
[23] Takata R, Wong VW. ASME Internal Combustion Engine Division 2006 Fall Technical Conference. 2006. 281-293.
[24] ASTM. ASTM D2270 Standard Practice for Calculating Viscosity Index from Kinematic Viscosity at 40 °C and 100 °C. ASTM Int 2016.
[25] Bartz WJ. Engine oils and automotive lubrication. CRC Press (1st edition), 1993.
[26] Hoshi M. Reducing friction losses in automobile engines. Tribology International. 1984:185–189.
[27] Kovach JT, Tsakiris EA. The Engineering Resource For Advancing Mobility Engine Friction Reduction for Improved Fuel Economy. SAE Tech Pap 1982.
[28] Hamatake T, Kitahara T, Wakuri Y, Soejima M. Friction characteristics of piston rings in a reciprocating engine. Lubr Sci 1993; 6:21–40.
[29] Rahmani R, Rahnejat H, Fitzsimons B, Dowson D. The effect of cylinder liner operating temperature on frictional loss and engine emissions in piston ring conjunction. Appl Energy 2017; 191:568–81.
[30] Shayler PJ, Leong DKW, Murphy M. Contributions to engine friction during cold, low speed running and the dependence on oil viscosity. SAE Tech Pap 2005.
[31] Ferguson CR KA. Internal Combustion Engines: Applied Thermosciences. John Wiley & Sons; 2015.
[32] Werner M, Merkle A, Graf S, Holzmüller R, Wachtmeister G. Calculation of the piston assembly friction: Classification, validation and interpretation. SAE Tech Pap 2012.
[33] Rakopoulos CD, Giakoumis EG. Prediction of friction development during transient diesel engine operation using a detailed model. Int J Veh Des 2007; 44:143–66.
[34] Abril SO, Rojas JP, Flórez EN. Numerical methodology for determining the energy losses in auxiliary systems and friction processes applied to low displacement diesel engines. Lubricants 2020; 8: 1–25.
[35] Taylor JR. Error analysis. Univ. Science Books, Sausalito, California. 1997.